

Numerical Dispersion

Learning Outcomes

Following this lecture, students will be able to:

- Describe the general procedure by which the dispersion properties of a given spatial and temporal finite difference approximation combination can be determined.

Review of Linear Numerical Stability

In previous lectures, we considered the linear numerical stability of advection and diffusion terms when approximated with spatial and temporal differencing schemes. For example, for advection, we considered a one-dimensional advection equation of the form:

$$\left. \frac{\partial h}{\partial t} \right|_j^\tau = -U \left. \frac{\partial h}{\partial x} \right|_j^\tau$$

We assumed that a model variable h has wave-like solutions of the form $h = \hat{h}e^{i(kx - \omega t)}$, where \hat{h} is amplitude, k is a zonal wavenumber, L is wavelength, and $\omega = Uk$ is frequency. The frequency has both real and imaginary components, i.e., $\omega = \omega_R + i\omega_I$, such that $h = \hat{h}e^{\omega_I t} e^{i(kx - \omega_R t)}$. Thus, the amplitude of h may change with time as a function of the value of $e^{\omega_I t}$.

We discretized this equation using various combinations of spatial and temporal finite difference approximations. The resulting equations were then solved for $|e^{\omega_I \Delta t}|$, noting that $e^{\omega_I t} = (e^{\omega_I \Delta t})^\tau$ since $t = \tau \Delta t$ and $\tau =$ time step number.

Intuitively, shorter-wavelength features – where Δx is large relative to their wavelength L – are poorly resolved on the model grid. As we will demonstrate in this lecture, shorter-wavelength features are also problematic with respect to their modeled propagation. This is known as **numerical dispersion**, describing non-physical wave and energy propagation that can result from finite differencing schemes.

The Mathematics of Numerical Dispersion

Consider the linear one-dimensional advection equation stated above. The advective speed of the wave defined by h is simply equal to U , a constant advective velocity. More precisely, the phase speed of any wave – defining its motion – is given by:

$$C_p = \frac{\omega}{k}$$

Here, since $\omega = Uk$, $C_p = U$. To prove this, consider the linear one-dimensional advection equation and the general solution for $h = \hat{h}e^{i(kx - \omega t)}$. Plugging this in and solving for the partial derivatives analytically, we obtain:

$$-i\omega\hat{h}e^{i(kx - \omega t)} = -ikU\hat{h}e^{i(kx - \omega t)}$$

Solving for ω , this simplifies to $\omega = Uk$.

Likewise, the group velocity – defining the propagation of the wave's energy – is given by:

$$C_g = \frac{\partial\omega}{\partial k}$$

Here, again since $\omega = Uk$, $C_g = U$. Because $C_p = C_g$, the wave is said to be *non-dispersive*, and this is true of any real-world advected wave.

However, when the solution to the advection equation is approximated using finite-difference schemes, the phase speed and group velocity may not necessarily equal U , nor will they necessarily equal each other. Rather,

$$C_p = \frac{\omega_R}{k} \quad \text{and} \quad C_g = \frac{\partial\omega_R}{\partial k}$$

For instance, consider the forward-in-time, backward-in-space finite-difference schemes applied to the one-dimensional advection equation. We previously found that:

$$e^{\omega_r\Delta t} (\cos(\omega_R\Delta t) - i \sin(\omega_R\Delta t)) - 1 = -\frac{U\Delta t}{\Delta x} (1 - (\cos(k\Delta x) - i \sin(k\Delta x)))$$

Separating this equation into its real (top) and imaginary (bottom) components, we obtained:

$$e^{\omega_r\Delta t} \cos(\omega_R\Delta t) = 1 - \frac{U\Delta t}{\Delta x} (1 - \cos(k\Delta x))$$

$$e^{\omega_r\Delta t} \sin(\omega_R\Delta t) = \frac{U\Delta t}{\Delta x} \sin(k\Delta x)$$

To evaluate the linear numerical stability, we solved the system of equations for $e^{\omega_r\Delta t}$ by eliminating ω_R . Now, to determine the phase speed and group velocity, we now wish to solve the system of equations for ω_R (which shows up in both C_p and C_g) by eliminating $e^{\omega_r\Delta t}$. We can do so by dividing the bottom equation by the top equation to obtain:

$$\frac{\sin(\omega_R \Delta t)}{\cos(\omega_R \Delta t)} = \frac{\frac{U \Delta t}{\Delta x} \sin(k \Delta x)}{1 - \frac{U \Delta t}{\Delta x} (1 - \cos(k \Delta x))}$$

To solve this equation for ω_R , note that the left-hand side of the above equation is simply equal to $\tan(\omega_R \Delta t)$. Thus, take the inverse tangent (or arctangent) of both sides to obtain:

$$\omega_R \Delta t = \arctan \left(\frac{\frac{U \Delta t}{\Delta x} \sin(k \Delta x)}{1 - \frac{U \Delta t}{\Delta x} (1 - \cos(k \Delta x))} \right)$$

For $\omega_R = C_p k$, we can rewrite the above equation as:

$$C_p = \frac{1}{k \Delta t} \arctan \left(\frac{\frac{U \Delta t}{\Delta x} \sin(k \Delta x)}{1 - \frac{U \Delta t}{\Delta x} (1 - \cos(k \Delta x))} \right)$$

This phase speed is not equal to U but is now dependent on the model time step Δt , the grid spacing Δx , and the wavelength L (since $k = 2\pi/L$), as visualized in Fig. 1.

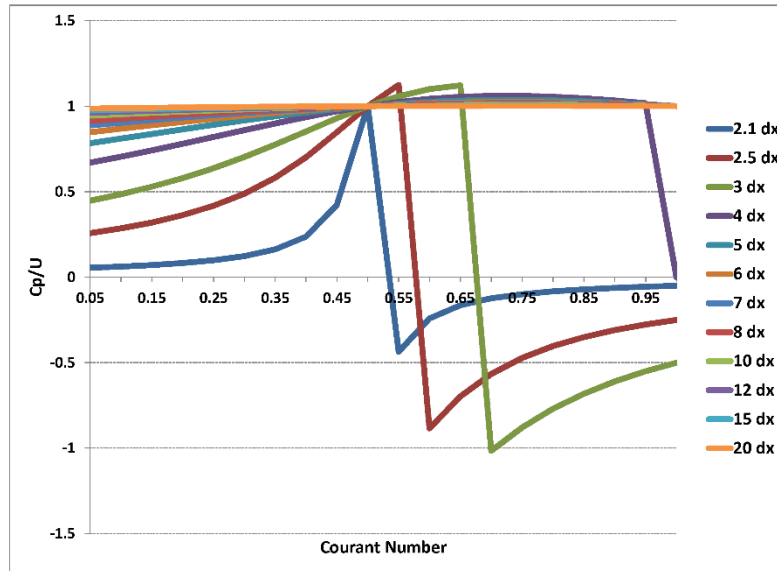


Figure 1. Ratio of the phase speed C_p to the advective velocity U for the forward-in-time, backward-in-space finite difference schemes for Courant numbers C between 0.05 and 1 and waves of wavelength between $2.1\Delta x$ and $20\Delta x$. Adapted from Warner (2011), their Fig. 3.24, with correct data plotted for wavelengths $\leq 4\Delta x$.

For this combination of spatial and temporal differencing schemes, the phase speed is slower than U for $C < 0.5$, equal to U for $C = 0.5$ and 1, and greater than U for $0.5 < C < 1$ for waves of wavelength $5\Delta x$ and longer. The phase speed is slower than U for $C < 0.5$ and equal to U for $C = 0.5$ for waves of wavelength $4\Delta x$ and shorter. However, $C > 0.5$, the phase speed can be negative or undefined.

The phase speed's dependency on wavelength indicates that the wave-like solution for h is *dispersive*. In general, a wave with a phase speed that depends on wavelength is dispersive. We will consider what this means conceptually with an example later in this lecture.

Similarly, one could take the equation for $\omega_R \Delta t$, solve it for ω_R , and then take its first partial derivative with respect to k to obtain an expression for C_g , the group velocity describing wave energy propagation. Doing so, one would find that $C_p \neq C_g$, such that the wave and its energy are associated with different propagation characteristics, a characteristic of a dispersive wave.

The process described above can be repeated for *any* combination of finite-difference schemes. For example, the centered-in-time, 2nd order centered-in-space finite difference scheme has the following dispersion relationship:

$$\omega_R \Delta t = \arcsin\left(\pm \frac{U \Delta t}{\Delta x} \sin(k \Delta x)\right)$$

Substituting for $\omega_R = C_p k$, we can rewrite the above as:

$$C_p = \frac{1}{k \Delta t} \arcsin\left(\pm \frac{U \Delta t}{\Delta x} \sin(k \Delta x)\right)$$

Because of the \pm symbol, there are two different phase speeds – for two different waves – defined above:

$$C_p = \frac{1}{k \Delta t} \arcsin\left(\frac{U \Delta t}{\Delta x} \sin(k \Delta x)\right)$$

$$C_p = \frac{1}{k \Delta t} \arcsin\left(-\frac{U \Delta t}{\Delta x} \sin(k \Delta x)\right)$$

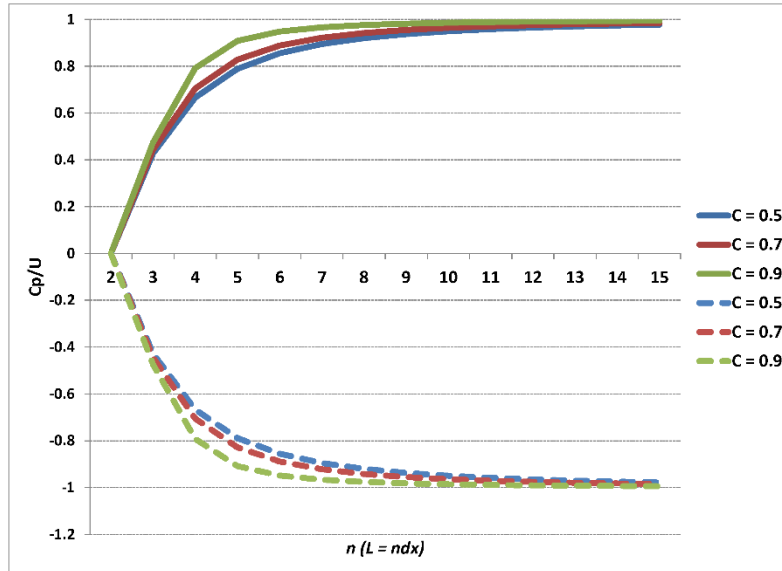


Figure 2. Ratio of the phase speed C_p to the advective velocity U for the centered-in-time, 2nd order centered-in-space finite-difference schemes as a function of wavelength for three selected values of the Courant number. Solid lines depict the phase speed of the approximation to the physical wave while dashed lines depict the phase speed of the computational mode. Adapted from Warner (2011), their Fig. 3.25.

The first approximates the physical wave that moves in the same direction as, but at a slower rate of speed than, the physical wave. The second is a fictitious wave, or *computational mode*, that moves in the opposite direction with smaller magnitude than the physical wave. The ratios of the phase speed C_p to the advective velocity U for each wave are plotted in Fig. 2. Note that the greatest departures from $|U|$ occur for $L < 8\Delta x$ and for smaller Courant numbers.

A temporal differencing scheme that involves computations at more than two times (e.g., the current and future times) is associated with one or more computational modes. For example, the centered-in-time temporal differencing scheme is second-order accurate – involving three times – and has one physical mode and one computational mode. The Runge-Kutta 3 temporal differencing scheme is third-order accurate – involving four times – and has one physical mode and two computational modes. In general, for a temporal differencing scheme that is N^{th} order accurate, involving $N+1$ times, there are $N-1$ computational modes.

The computational mode(s) typically have much smaller amplitude than does the physical mode, and it can be difficult to isolate the impact of the computational mode on the numerical solution from that of numerical dispersion. As depicted above, wave dispersion is most evident for shorter wavelength features; this is generally true for computational mode solutions as well.

Typically, both computational mode and short wavelength dispersive waves are dampened in the model solution by implicit and/or explicit numerical diffusion. Time filtering may also be used to mitigate the computational mode, but this typically also reduces the temporal differencing scheme's accuracy and is associated with a more stringent stability criterion.

Returning to the centered-in-time, second-order centered-in-space differencing schemes, we can obtain the group velocity C_g for the approximation to the physical wave:

$$C_g = \frac{\partial \omega_R}{\partial k} = \frac{\partial(C_p k)}{\partial k}$$

If we plug in for C_p , we obtain:

$$C_g = \frac{\partial}{\partial k} \left(\frac{1}{\Delta t} \arcsin \left(\frac{U \Delta t}{\Delta x} \sin(k \Delta x) \right) \right)$$

Noting that:

$$\frac{\partial}{\partial k} \arcsin(a(k)) = \frac{1}{\sqrt{1-a^2}} \frac{\partial a}{\partial k}$$

we obtain:

$$C_g = \frac{1}{\Delta t} \left(\frac{1}{\sqrt{1 - \left(\frac{U \Delta t}{\Delta x} \sin(k \Delta x) \right)^2}} \right) \frac{\partial}{\partial k} \left(\frac{U \Delta t}{\Delta x} \sin(k \Delta x) \right)$$

Such that:

$$C_g = \frac{1}{\Delta t} \left(\frac{\frac{U \Delta t}{\Delta x} \Delta x \cos(k \Delta x)}{\sqrt{1 - \left(\frac{U \Delta t}{\Delta x} \sin(k \Delta x) \right)^2}} \right)$$

Simplifying, we obtain:

$$C_g = \left(\frac{U \cos(k\Delta x)}{\sqrt{1 - \left(\frac{U\Delta t}{\Delta x} \sin(k\Delta x) \right)^2}} \right)$$

The ratio of the group velocity to the advective velocity is depicted in Fig. 3. The group velocity and phase speed are not equal (c.f. Figs. 2 and 3), such that the computational representation of the wave with this combination of differencing schemes is dispersive. For $L < 4\Delta x$, the group velocity is in the opposite direction of the wave's propagation. For $L = 4\Delta x$, the group velocity is stationary. For $L > 4\Delta x$, the group velocity is in the same direction as but slower than the wave's propagation, particularly for $L < \sim 10\Delta x$. As with phase speed, the greatest departures from $|U|$ occur for smaller values of the Courant number.

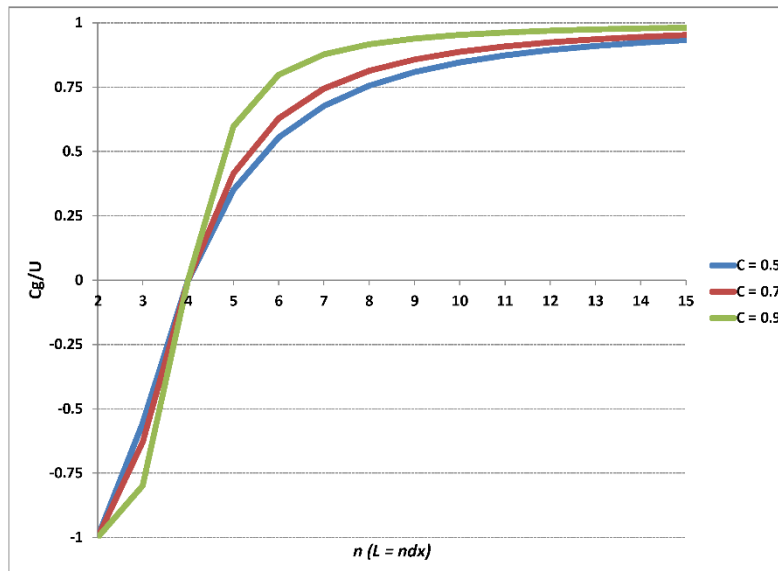


Figure 3. Ratio of the group velocity C_g to the advective velocity U for the centered-in-time, 2nd order centered-in-space finite difference scheme applied to the one-dimensional advection equation as a function of wavelength for three selected values of the Courant number. Adapted from Warner (2011), their Fig. 3.25.

Note that the wavelength- and Courant number-dependence of C_p and C_g varies between finite differencing schemes.

An Idealized Example

Consider a model that solves the one-dimensional advection equation given by:

$$\frac{\partial h}{\partial t} = -U \frac{\partial h}{\partial x}$$

Let the model grid contain 100 grid points. Use periodic boundary conditions, such that grid point 1 is adjacent to grid points 100 and 2, and grid point 100 is adjacent to grid points 99 and 1. Here, we let $\Delta x = 1$ km (such that the domain length is 100 km) and $U = 10$ m s⁻¹. The initial h is defined by a short wavelength Gaussian wave, with high amplitude for large k and low amplitude for small k , in the height field at the center of the model grid.

We consider three model time steps: $\Delta t = 10$ s, such that $C = 0.1$; $\Delta t = 50$ s, such that $C = 0.5$; and $\Delta t = 90$ s, such that $C = 0.9$. In each case, the model is integrated forward in time until the Gaussian-like wave returns to its original location (at $t = 100000$ m / 10 m s⁻¹ = 10000 s); thus, the exact solution is identical to the initial condition. Centered-in-time, second-order centered-in-space finite differencing schemes are used for each integration; as a result, there is no implicit damping of the model solution with time for any value of C .

In Fig. 4, the approximate solution for each of the above-listed Courant numbers is depicted. The initial condition and exact solution are given by the thin grey line in the top panel. From Fig. 2, we know that the phase speed is wavelength-dependent: shorter-wavelength features move at a slower rate of speed than the longer-wavelength features. For *all* wavelengths, this effect is smallest when the Courant number is close to 1 and is largest for small Courant numbers.

Now, consider the cases where $C = 0.1$ but centered-in-time, fourth-order centered-in-space (Fig. 5) and Runge-Kutta 3, sixth-order centered-in-space (Fig. 6) differencing schemes are used. The former contains no implicit damping, whereas the latter does due to the Runge-Kutta temporal differencing (the sixth-order spatial-differencing scheme does not implicitly dampen). Short-wavelength features move slower than the physical wave in both cases; however, this effect is less pronounced with these higher-order-accurate schemes, better preserving the primary wave's amplitude and appearance. Thus, using more-accurate finite difference schemes in both time and space mitigates the deleterious effects of numerical dispersion on the model solution.

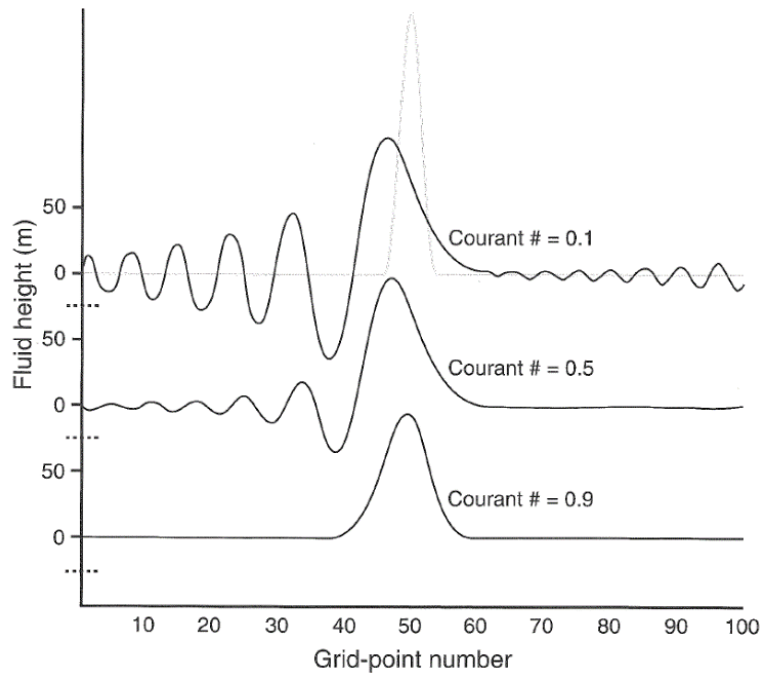


Figure 4. Fluid height h (m) after integrating the one-dimensional advection equation for 10,000 s on the model grid described in the text above for Courant numbers C of 0.1 (top), 0.5 (middle), and 0.9 (bottom). The thin grey curve in the top panel represents both the initial condition and exact solution. Reproduced from Warner (2011), their Fig. 3.27.

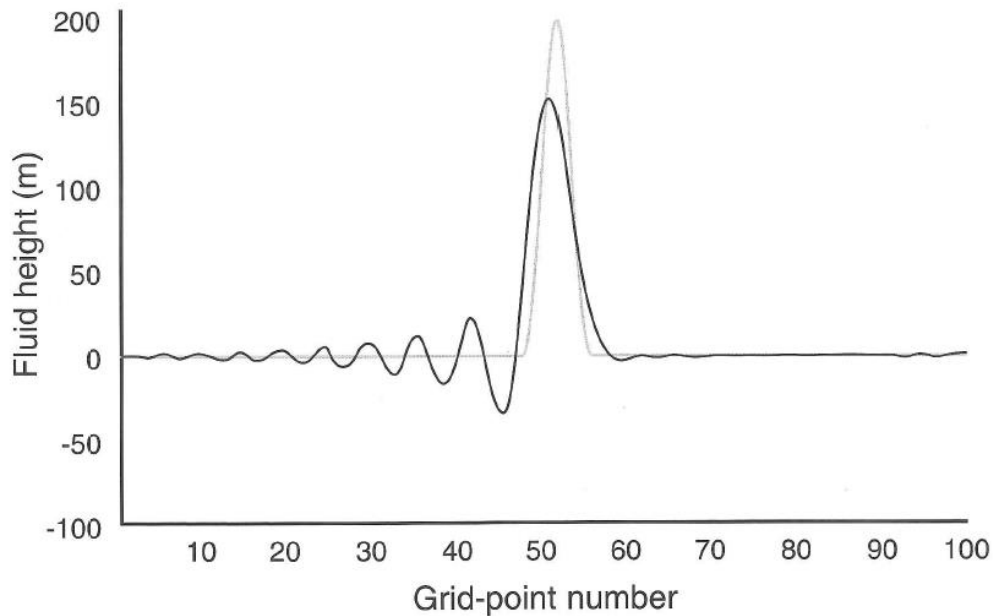


Figure 5. As in the top panel of Fig. 4, except using the centered-in-time, fourth-order centered-in-space finite differencing scheme. Reproduced from Warner (2011), their Fig. 3.28.

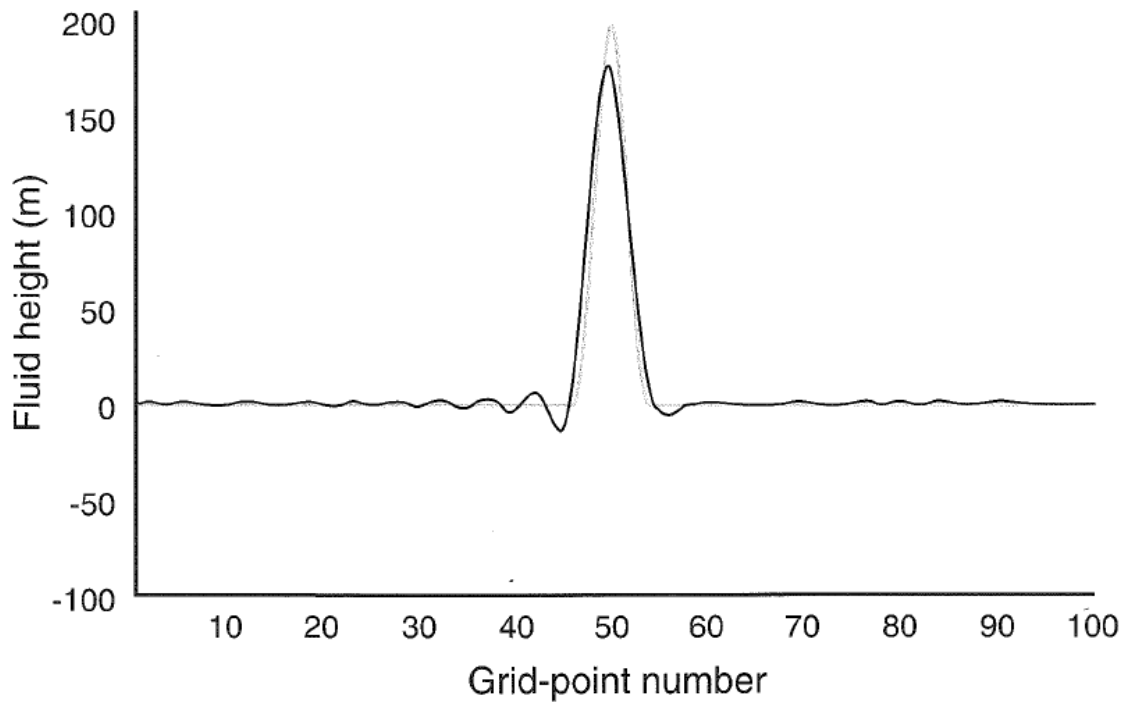


Figure 6. As in the top panel of Fig. 4, except using the third-order Runge-Kutta in time, sixth-order centered-in-space finite differencing scheme. Reproduced from Warner (2011), their Fig. 3.30.